IIETA International Information and Engineering Technology Association
Advancing the World of Information and Engineering

Mathematical Modelling of Engineering Problems
Vol. 12, No. 12, December, 2025, pp. 4257-4266
Journal homepage: http://iieta.org/journals/mmep

An Investigation on a Theoretical Model for Predicting a Cassava Peeler's Useful Flesh Recovery

Charles Olawale Ogunnigbo*, Lodewyk Willem Beneke, Christiaan Coenrad Oosthuizen

Department of Mechanical and Mechatronics Engineering, Faculty of Engineering and Built Environment, Tshwane University of Technology, Pretoria 0183, South Africa

Corresponding Author Email: charles_olawale@yahoo.com

https://doi.org/10.18280/mmep.121214

Received: 2 September 2025
Revised: 28 October 2025
Accepted: 3 November 2025
Available online: 31 December 2025

Keywords:
cassava peeling, predictive modelling, useful flesh recovery, dimensional analysis, engineering design

ABSTRACT

This study presents a predictive model for estimating the useful flesh recovery of cassava during the peeling process. By employing a dimensional analysis approach, the model identifies key factors that influence the effectiveness of cassava peelers. Our findings demonstrate a strong correlation between experimental and predicted results, achieving a coefficient of determination (R^2) of 0.9754 with a Root Mean Square Error (RMSE) of 0.01, indicating high accuracy. The model highlights several optimal variables, such as tuber size, peel thickness, and friction coefficients, which significantly impact the recovery of useful flesh. These insights are crucial for improving the design and efficiency of cassava peeling machines, ultimately reducing waste and enhancing productivity in cassava processing. Incorporating this model into engineering practices allows designers to optimize peeling performance, paving the way for more efficient cassava processing solutions. This research underscores the importance of predictive modeling in agricultural engineering, providing valuable tools for enhancing food production systems.

1. INTRODUCTION

Efficient mechanization can significantly reduce the drudgery associated with post-harvesting processes. In cassava processing, peeling is a critical step, influencing the recovery of useful flesh and overall product quality [1]. Despite ongoing technological advancements, peeling continues to pose a global challenge in cassava processing due to several factors. One major issue is the high variability in tuber size and shape, which complicates the peeling process and makes it difficult to design a one-size-fits-all solution [2, 3]. Additionally, the peel adherence to the flesh can vary significantly among different cassava varieties, leading to inconsistent peeling efficiency and increased waste. Furthermore, the moisture content and texture of the tubers can also influence the effectiveness of peeling methods. As noted by Krishnakumar et al. [4], these challenges necessitate continued innovation in peeling technologies. Additionally, Amuda and Alabdulrahman [5] highlight the importance of cassava production for enhancing food security and facilitating industrialization and foreign exchange. Therefore, there is an urgent need for innovative technologies and methodologies to enhance the effectiveness of cassava processing.

The performance of peeling systems can be effectively modeled to predict their functional behavior. Researchers employ numerical analysis [6-8] and computational fluid dynamics [9-13] to tackle complex problems. However, empirical data is often necessary to validate theoretical models, underscoring the importance of experiments in addressing practical challenges [8, 14].

Mathematical modeling serves as a theoretical framework to represent real-world phenomena, often generating predictive insights. Techniques such as dimensional analysis simplify complex physical problems, aiding in the design and scaling of experiments [15, 16]. While widely used in chemical and fluid dynamics, dimensional analysis is less prevalent in systems engineering. It offers a systematic approach to organizing and interpreting results, facilitating the transition from models to prototypes [17, 18].

Theoretical modeling in agricultural engineering has addressed various processes, including harvesting [19], sprayers [20], and crop handling systems [21]. However, data are scarce on modeling the useful flesh recovery of cassava. Previous works have explored related cutting processes, such as the impact on forage crops [22] and the efficiency of potato peeling [23, 24].

Dimensional analysis, particularly Buckingham's pi theorem, has proven effective in developing predictive models across engineering domains, including micro-channel heat sinks [25], ball bearing parameters [26], scaling-up simulation of Proton Exchange Membrane Fuel Cells impedance [27], scaling up direct contact membrane distillation processes [28], cassava peelers [29], ARD plow drag force in silty clay medium [30], and multi-effect vacuum membrane distillation systems integrated with Organic Rankin Cycle and PVT [31].

Given its significance for accurate system predictions, this study aims to establish a numerical framework for predicting useful flesh recovery in a cassava peeling process. By

leveraging dimensional analysis, the research seeks to optimize equipment efficiency and enhance outcomes within the broader cassava processing industry, ultimately contributing to improved productivity and reduced waste.

2. MATERIALS AND METHODS

2.1 Conceptual approach

In the development of the model, the relationship between the independent and dependent parameters was ascertained with a view to estimating which parameter affects the performance of a developed machine. Dimensional analysis was adopted as an approach that is utilized in determining elements that go into an actual condition and establishing a functional correlation among them.

Nevertheless, dimensional analysis, which is based on Buckingham's π theorem, establishes that, in the case of a functional relationship with m variables and n total dimensions, the functional correlation will include m – n groups of dimensionless quantities when dimensional analysis is applied [32].

Given that the functional relationship of the model consists of $x_1, x_2, \dots x_m$ variables irrespective of which is the dependent quantity, the functional relationship can be expressed as:

$$f(x_1, x_2, \dots x_m) = 0 \tag{1}$$

Given that variables have *n* basic dimensions altogether, then the procedure for dimensional analysis will transform the functional relationship into:

$$f_1(\pi_1, \pi_2, \dots \pi_{m-n}) = 0 \tag{2}$$

In determining the number of pi's, the repeating variables are identified as *n*, which must together contain the *n* basic dimensions:

$$\therefore \pi_1 = \left(x_1^{y11}, x_2^{y12} \dots x_n^{y1n}\right) x_{n+1} \tag{3}$$

$$\pi_2 = \left(x_1^{y21}, x_2^{y22} \dots x_n^{y2n}\right) x_{n+2} \tag{4}$$

$$\pi_{m-n} = \left(x_1^{y(m-n)1}, x_2^{y(m-n)2} \dots x_n^{y(m-n)n}\right) x_m \tag{5}$$

The variables are represented based on the basic dimensions for each equation; the π is similarly expressed while each of the basic dimensions is raised to the power of zero [33]. The equations are thereafter resolved by setting to zero the exponent of each basic dimension.

2.2 Model development assumptions

In the development of the model, some simplifying assumptions were made.

- Consideration was not given to variables that are functions of other variables, such as time, which is a function of tuber speed of rotation. Moreso, peel penetration force is time-dependent instead of acceleration.
- Tuber orientation, age, and variations are considered negligible in the development of the model.
- Consideration was given to measurable design parameters and variables.

2.3 Development of the functionally useful flesh recovery equation

After some analysis, we have identified the core variables that significantly influence the recovery of useful flesh from cassava tubers. These variables encompass various physical and operational factors that affect the peeling process. The functional relationship among these variables is captured in our predictive model, which aims to estimate the useful flesh recovery based on their interactions. The stated assumptions assisted in minimizing the quantity of variables that are available to the ones highlighted as they were taken into consideration to have a significant impact on the useful flesh recovery on the selected cassava tuber and are quantifiable. The variables include; proportion by weight of peel (W_p), Size of tuber (L_t), tuber speed of rotation (ω), peel shear stress (τ), cutting tool thickness (t_{ct}), moisture content of tuber (φ), coefficient of friction between the peel and peeling tool (μ), peel penetration force (F), shape of the tuber (γ), and the thickness of the peel (t_p).

Having identified the core variables influencing the useful flesh recovery of the tuber, Eq. (6) describes the predictive framework's functional equation.

$$U_{fr} = f\left(\mu, \gamma, W_p, L_t, t_p, F, \tau, \varphi, \omega, t_{ct}\right) \tag{6}$$

where, U_{fr} is the useful flesh recovery.

Table 1. List of variables and dimensions

S/N	Variable	Symbol	Unit	Dimensions
1	Useful flesh recovery	U_{fr}	%	$M^0L^0T^0$
2	Coefficient of friction	μ	μ	$M^0L^0T^0$
3	Size of tuber	L	m	L
4	Peel thickness	t_p	m	L
5	Peel penetration force	F	kgs^{-2}	MT^{-2}
6	Moisture content	φ	φ	$M^0L^0T^0$
7	Peel shear stress	τ	$kgs^{-2}m^{-2}$	$ML^{-1}T^{-2}$
8	Angular speed	ω	rpm	T^{-1}
9	Cutting tool thickness	t_{ct}	m	L
10	Shape of the tuber	γ	γ	$M^0L^0T^0$
11	Proportion by weight of peel	W_p	W_p	$M^0L^0T^0$

Table 2. Variable-dimensional matrix

S/N	Variable	Symbol	M	L	T
1	Useful flesh recovery	U_{fr}	0	0	0
2	Coefficient of friction	μ	0	0	0
3	Size of tuber	L_t	0	1	0
4	Peel thickness	t_p	0	1	0
5	Angular speed	ω	0	0	-1
6	Peel penetration force	F	1	0	-2
7	Moisture content	φ	0	0	0
8	Peel shear stress	τ	1	-1	-2
9	Cutting tool thickness	t_{ct}	0	1	0
10	Shape of the tuber	γ	0	0	0
11	Proportion by weight of peel	W_p	0	0	0

Using the [*T*], [*L*], and [*M*] system of dimension [34, 35], the variable dimensions are represented in Table 1, while Table 2 presents the dimensional matrix of the model. From Buckingham's π theorem [32], the total number of dimensionless quantities (*n*) to be generated is presented as:

$$n = X - x \tag{7}$$

where, X = Number of variables under consideration = 11; x = Number of fundamental dimensions specifying the variables = 3. Hence, n = 11 – 3 = 8.

Eight dimensionless quantities were created, signifying the need to form $\pi_1;\ \pi_2; \pi_3;\ \pi_4; \pi_5; \pi_6, \pi_7\ and\ \pi_8$ in describing the system.

From Table 2, it can be observed that $U_{fr}, W_p, \gamma, \mu,$ and φ are dimensionless and hence not included from the dimensionless terms estimation which is to be added thereafter [36] while the other variables are combined to create the pi terms. Speed of tuber rotation (ω), peel penetration force (F) and tuber size (L_t) were chosen as the set of criteria that would be used repeatedly since they constitute all the main dimensions present in the problem and their respective combinations do not form a dimensionless term.

In our modeling approach, we have identified three key variables; angular velocity ω, applied force F, and tuber length L_t as the primary recurring sets in the predictive framework. To establish a relationship that allows for dimensional analysis, we assign exponents a, b and c to these variables, respectively. By taking the product $\omega^a F^b L_t^c$ and dividing it by the remaining variables, peel shear stress (τ), cutting tool thickness (t_{ct}), and thickness of the peel (t_p). We derive a set of dimensionless groups.

These dimensionless groups, denoted as $\pi_1,\ \pi_2,$ and π_3, facilitate the analysis of the system by reducing the number of variables and allowing for a clearer understanding of their relationships [36-39]. The resulting dimensionless groups are presented in the following Eqs. (8)-(15) below:

Hence,

$$\pi_1 = \frac{t_{ct}}{L_t} \tag{8}$$

$$\pi_2 = \frac{t_p}{L_t} \tag{9}$$

$$\pi_3 = \frac{\tau L_t}{F} \tag{10}$$

$$\pi_4 = U_{fr} \tag{11}$$

$$\pi_5 = W_p \tag{12}$$

$$\pi_6 = \varphi \tag{13}$$

$$\pi_7 = \mu \tag{14}$$

$$\pi_8 = \gamma \tag{15}$$

Eq. (16) was then established by combining the equations given above, whose constituents are dimensionless and given as:

$$\begin{aligned} \pi_1 &= f(\pi_2;\ \pi_3;\ \pi_4;\ \pi_5;\ \pi_6; \pi_7;\ \pi_8) \\ \therefore \frac{t_{ct}}{L_t} &= f\left(\frac{t_p}{L_t}, \frac{\tau L_t}{F}, U_{fr}, W_p, \mu, \varphi, \gamma\right) \end{aligned} \tag{16}$$

Eqs. (17)-(20) are dimensionless, and they are obtained by multiplying and/or dividing the dimensionless quantities to bring them down to a practicable point [40].

$$\pi_{12} = \frac{\pi_1}{\pi_2} = \frac{t_{ct}}{t_p} \tag{17}$$

$$\pi_3 = \frac{\pi_3}{1} = \frac{\tau L_t}{F} \tag{18}$$

$$\pi_{56} = \frac{\pi_5}{\pi_6} = \frac{W_p}{\varphi} \tag{19}$$

$$\pi_{78} = \frac{\pi_7}{\pi_8} = \frac{\mu}{\gamma} \tag{20}$$

The new dimensionless functional relationship yields Eqs. (21) and (22) given as:

$$\pi_{12} = f(\pi_3, \pi_{56}, \pi_{78}) \tag{21}$$

$$\frac{t_{ct}}{t_p} = f\left(\frac{\tau L_t}{F}, \frac{W_p}{\varphi}, \frac{\mu}{\gamma}\right) \tag{22}$$

$$\therefore t_{ct} = t_p\, f\left(\frac{\tau L_t}{F}, \frac{W_p}{\varphi}, \frac{\mu}{\gamma}\right) \tag{23}$$

Hence, by further simplifying Eq. (23), we obtained Eq. (24):

$$t_{ct} = f\left(\frac{\tau L_t t_p}{F}, \frac{W_p t_p}{\varphi}, \frac{\mu t_p}{\gamma}\right) \tag{24}$$

Building upon our earlier analysis and the dimensionless groups derived, we can further express the useful flesh recovery U_{fr} in a more detailed form. From Eq. (24), we can manipulate the relationships among the identified variables to derive a specific expression for U_{fr}. This expression captures the interplay of shear stress, tuber length, peeling time, applied force, weight of the tuber, moisture contents, friction, and the angle of the peeling tool.

The resulting expression for U_{fr} is given by Eq. (25):

$$U_{fr} = f\left(\frac{\tau L_t t_p}{F t_{ct}}, \frac{W_p t_p}{\varphi t_{ct}}, \frac{\mu t_p}{\gamma t_{ct}}\right) \tag{25}$$

Eq. (25) describes the expression for useful flesh recovery U_{fr} with the parameters as a function of three functional quantities; $\frac{\tau L_t t_p}{F t_{ct}}$, $\frac{W_p t_p}{\varphi t_{ct}}$ and $\frac{\mu t_p}{\gamma t_{ct}}$ which are characterised as P, Q and R respectively in Eq. (26):

$$U_{fr} = f(P, Q, R) \tag{26}$$

2.4 Experimental assessment

Twenty samples of fully grown two-year-old TME 419 variety of cassava tubers (*Manihot Esculenta Crantz*) harvested from Obafemi Awolowo University, Ile – Ife, Nigeria, Teaching and Research Farm were sorted into different units after being completely cleaned of all contaminants to determine some physical characteristics of cassava tubers that would be needed for developing the model. A computer vision driven approach was utilized as a means for driving a peeling knife at a preset speed of 0.33 mm/s, which moves through a span of 0.2 m and penetrates the tuber up to the peel thickness layer (Cambium) and peels the tuber

specimen, which revolves against a fixed peeling tool. Figure 1 describes the peeling mechanism experimental setup.

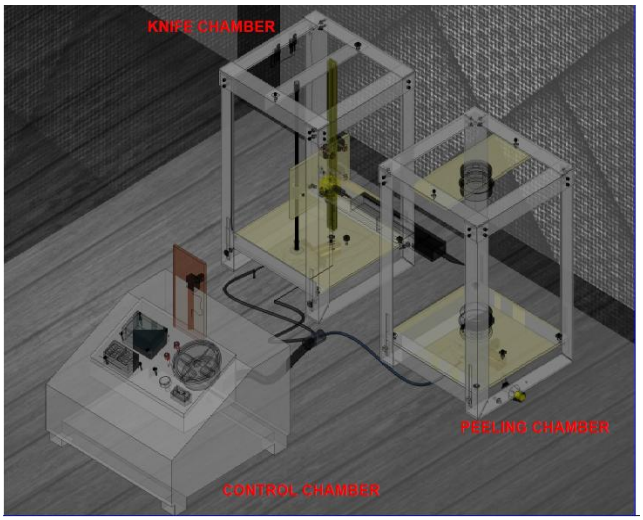

Figure 1. Empirical arrangement of the peeling mechanism for estimating the useful flesh recovery

Experimental results obtained from the peeling mechanisms are utilized in verifying the useful flesh recovery. Some apparatus used in empirical analysis are described below:

- Useful Flesh Recovery Measurement: Useful flesh recovery was estimated by weighing the flesh that was cut off in the process of peeling; afterward, the tuber's entire weight was calculated, estimated in %.
- Mass determination: An electronic weighing balance of sensitivity 0.01 g and ranging between 0.01 g and 5000 g was utilized in determining the mass of the tuber.
- Moisture content measurement: The tuber peel's moisture content was determined using the ASABE standard. This is with the view of understanding the extent of tool penetration into the inner layer of the tuber. The percentage of moisture content on a wet basis was calculated.
- Axial measurement: Linear measurement was made using a digital Vernier Calliper and measuring tape.

2.5 Input parameter for model and validation

By varying the sizes of tuber while maintaining the other parameters indicated in Table 3, the validation parameters were established. Applying the empirical values obtained and results by Adetan et al. [41]. Table 3 describes the values utilized in predicting the useful flesh recovery of the tuber.

Table 3. Evaluation parameters [42-44]

S/N	Variables	Value
1	Peel penetration force (N/mm)	1.02–1.21
2	Coefficient of friction	0.38–0.65
3	Peel thickness (mm)	2.12–2.94
4	Size of tuber (mm)	115.00–362.00
5	Peel shear stress (N/mm^2)	0.88–6.05
6	Moisture content	63.00–70.00
7	Cutting tool thickness (mm)	1.50–2.97
8	Shape of the tuber	0.62–0.84
9	Proportion by weight of peel	0.11–0.17

The predicted useful flesh recovery equation was established by making one of the useful flesh recovery groups $P\left(\frac{\tau L_t t_p}{F t_{ct}}\right)$, $Q\left(\frac{W_p t_p}{\varphi t_{ct}}\right)$ or $R\left(\frac{\mu t_p}{\gamma t_{ct}}\right)$ to change at a time while maintaining others constant and noting the resulting change in functions [40]. This was obtained by plotting the empirical results of U_{fr} against $P = \left(\frac{\tau L_t t_p}{F t_{ct}}\right)$ while maintaining Q and R as constant quantities. $P = \left(\frac{\tau L_t t_p}{F t_{ct}}\right)$ was estimated through substitution of established quantities (as given in Table 3 above) for peel shear stress (τ), tuber size (L_t), thickness of the peel (t_p), peel penetration force (F), and cutting tool thickness (t_{ct}) into P. Also, U_{fr} against $Q = \left(\frac{W_p t_p}{\varphi t_{ct}}\right)$ was plotted maintaining P and R constant while the same was done for $R = \left(\frac{\mu t_p}{\gamma t_{ct}}\right)$ maintaining P and Q as constant variables. In estimating the Useful Flesh Recovery for P, Q and R, the tuber size was varied while other parameters were kept constant [36, 40]. The established quantities for predicting useful flesh recovery were plotted against the measured (experimental) results for a regression analysis using a statistical package in Microsoft Excel 2010 and the coefficient of determination (R^2). The goodness of fit (suitability) or validity of the established model for the useful flesh recovery of selected cassava tubers was equally considered, and was tested by comparing with experimental results. Obtained R^2 indicates the suitability of the established framework.

3. RESULTS AND DISCUSSIONS

Table 4 presents the empirical results of the useful flesh recovery obtained from the computer vision assisted peeling mechanism and the predicted useful flesh recovery achieved by substituting values of the peeling parameters into the useful flesh equations $P = \left(\frac{\tau L_t t_p}{F t_{ct}}\right)$, $Q = \left(\frac{W_p t_p}{\varphi t_{ct}}\right)$ and $R = \left(\frac{\mu t_p}{\gamma t_{ct}}\right)$ respectively. Table 4 indicates a direct correlation between $\left(U_{fr(measured)}\right)$ and the predicted quantities (P, Q, R).

The $\left(U_{fr(measured)}\right)$ against P, Q and R are presented in Figures 2-4 respectively with their linear relationships and R^2 results expressed in Eqs. (27)-(29).

Hence,

$$U_{fr} = 0.0001P + 0.0727R^2 = 0.9471 \quad (27)$$

$$U_{fr} = 0.7628Q + 0.0726R^2 = 0.9470 \quad (28)$$

$$U_{fr} = 0.2373R + 0.0731R^2 = 0.9477 \quad (29)$$

Maintaining P and Q as constant variables, the plots of P, Q and R terms in Figures 2-4 generate a plane surface in linear space which indicates that their combinations favours addition or deduction or some forms of reconstruction between the established parameters [45, 46]. Hence, the component equations generated by the addition and subtraction of Eqs. (27)-(29) respectively yields.

$$\therefore U_{fr} = f_1(P,Q,R) - f_2(P,Q,R) - f_3(P,Q,R) + K \quad (30)$$

$$\therefore U_{fr} = f_1(P,Q,R) + f_2(P,Q,R) + f_3(P,Q,R) + K \quad (31)$$

It must be observed that at f_1, Q and R are viewed as constant parameters while P varies, at f_2, P and R are taken as constant as Q changes, and at f_3, P and Q are kept as constant quantities as R changes.

Table 4. Empirical results $\left(U_{fr(measured)}\right)$ and predicted quantities (P, Q, R) of useful flesh recovery of cassava

S/N	Peel Thickness (mm)	Measured (U_{fr})	P = $\left(\frac{\tau L_t t_p}{F t_{ct}}\right)$	Q = $\left(\frac{W_p t_p}{\varphi t_{ct}}\right)$	R = $\left(\frac{\mu t_p}{\gamma t_{ct}}\right)$
1	2.59	0.3122	2343.95	0.31859	1.022
2	2.69	0.3261	2434.45	0.33087	1.0616
3	2.79	0.3384	2524.95	0.34317	1.101
4	2.89	0.3459	2615.45	0.35547	1.141
5	2.99	0.3492	2705.95	0.36777	1.18

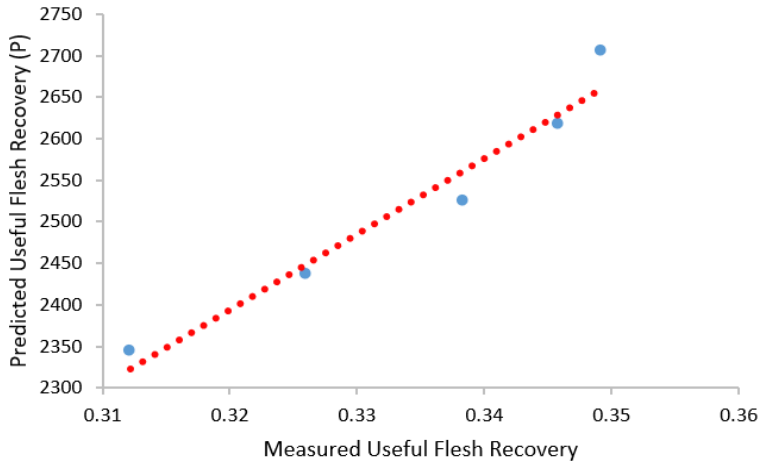

Figure 2. Variation of useful flesh recovery against P = $\left(\frac{\tau L_t t_p}{F t_{ct}}\right)$ keeping Q and R constant

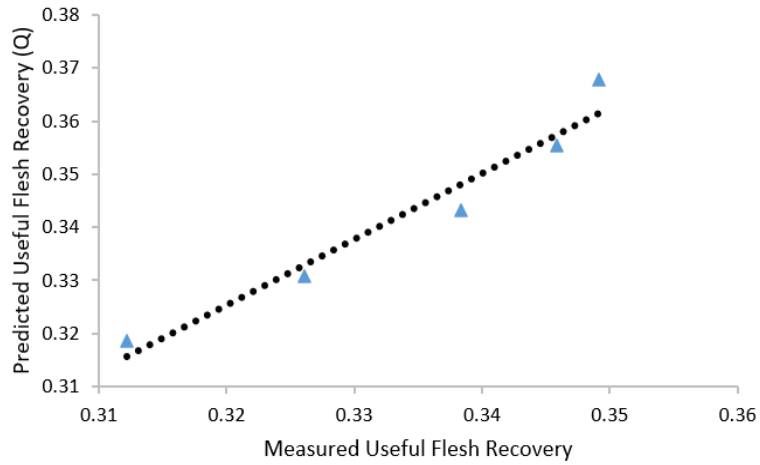

Figure 3. Variation of useful flesh recovery against Q = $\left(\frac{W_p t_p}{\varphi t_{ct}}\right)$ keeping P and R constant

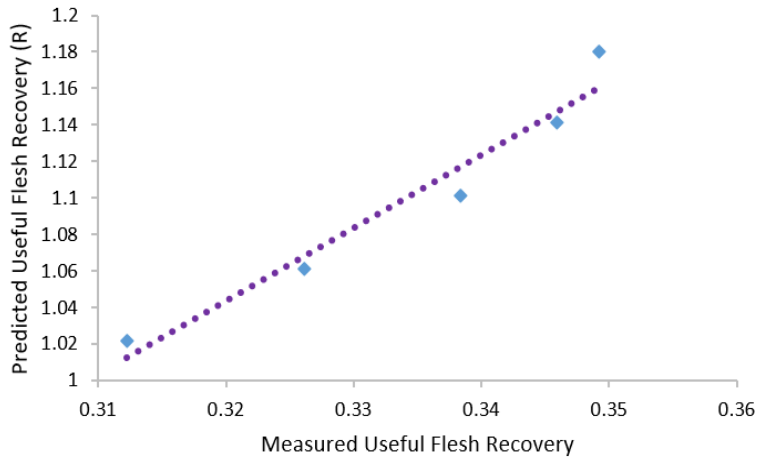

Figure 4. Variation of useful flesh recovery against R = $\left(\frac{\mu t_p}{\gamma t_{ct}}\right)$

Substituting Eqs. (27)-(29) into Eq. (30) and establishing some algebraic manipulations results in Eq. (32). This was necessary in order to create a more comprehensive framework that captures the interactions among different variables influencing useful flesh recovery.

$$U_{fr} = 0.0001P - 0.7628Q - 0.2373R - 0.073 \quad (32)$$

Also substituting the same equation into Eq. (31) gives:

$$U_{fr} = 0.0001P + 0.7628Q + 0.2373R + 0.2184 \quad (33)$$

In this study, we further refined our model by applying Buckingham's π theorem [40]. After a careful preliminary analysis and adjustments based on significance and impact on the model's performance, we introduced constant factors of -13.4 and 5 to modify Eqs. (32) and (33). By adjusting these constants, we can better align the model outputs with observed values, thereby improving the fit of the model to the data. This process is essential for capturing the inherent variability in the peeling process that may not be fully explained by the independent variables alone. This manipulation yields the following predicted model equations:

$$U_{fr} = -0.0065P + 2.0443Q + 0.6360R + 0.1956 \quad (34)$$

$$U_{fr} = 0.0025P + 0.7628Q + 0.2373R - 0.2184 \quad (35)$$

The incorporation of these constants enables a more accurate representation of the underlying phenomena. This is intended to refine the model's fit to the empirical data, ensuring that the combined equations align more closely with observed results.

Inputting the expressions for *P*, *Q* and *R* into the Eqs. (34) and (35) above yields:

$$U_{fr} = -0.0065\left(\frac{\tau L_t t_p}{F t_{ct}}\right) + 2.0443\left(\frac{W_p t_p}{\varphi t_{ct}}\right) + 0.6360\left(\frac{\mu t_p}{\gamma t_{ct}}\right) + 0.1956 \quad (36)$$

$$U_{fr} = 0.0025\left(\frac{\tau L_t t_p}{F t_{ct}}\right) + 0.7628\left(\frac{W_p t_p}{\varphi t_{ct}}\right) + 0.2373\left(\frac{\mu t_p}{\gamma t_{ct}}\right) - 0.2184 \quad (37)$$

Therefore, one of the two equations that produces superior inference from statistics will serve as the final projected model equation.

3.1 Validation of the model

The dataset was divided into training and testing subsets. The model was calibrated using 70% of the data, while the remaining 30% served as an independent validation set. This approach allowed us to assess the model's predictive performance on unseen data. We implemented k-fold cross-validation, where the data was partitioned into k subsets (k = 5). The model was trained on k-1 subsets and validated on the remaining subset iteratively. Also, the Root Mean Square Error (RMSE) was utilized in checking the error difference in the model.

Hence, model validation was carried out using five levels of tuber sizes varying from 121.8 to 260 mm at constant tuber rotation. A regression analytical technique as calculated using Microsoft Excel package was utilized in describing the functional relationship, plot the graphs and estimate the R^2.

Experimental results of variables were inputted into Eqs. (36) and (37) to generate the predicted useful flesh recovery results as plotted against the empirical data on a regression analysis so as to obtain the R^2 as presented in Figures 5 and 6 respectively. Eqs. (36) and (37) define the correlation that exist between the experimental and the predicted useful flesh recovery data with a high correlation R^2 values of 0.9752 and 0.9754 with RMSE values of 0.021 and 0.01, respectively.

High R^2 and low RMSE values for each of the predicted equations show that the approach used to develop the theoretical model is appropriate and will be effective for various tubers.

The theoretical equation reveals a significant effect of peel thickness on useful flesh recovery, validating the critical role of the processing variables in the peeling process. For instance, a thicker peel necessitates more force and time for removal, which directly impacts the amount of useful flesh recovered. This affirms the importance of designing peeling mechanisms that accommodate varying peel thicknesses to optimize recovery.

Additionally, the weight of the tuber W_p influences the gravitational force acting on the tuber, affecting its stability during peeling. Heavier tubers may require stronger holding mechanisms to prevent slippage, which is essential for maintaining consistent contact with the peeling tool. The model's significant coefficient for this parameter highlights that variations in tuber weight can lead to noticeable changes in flesh recovery, suggesting the need for adjustable designs that accommodate different sizes. The friction coefficient μ is another critical parameter, representing the interaction between the tuber surface and the peeling tool. A higher friction coefficient can enhance peeling effectiveness by ensuring better contact but may also increase wear on the tool. The predictive model emphasizes the necessity of optimizing friction, indicating that material selection for the peeling tool is vital for enhancing recovery rates.

Cutting tool thickness (t_{ct}), and thickness of the peel (t_p) are crucial in determining the effectiveness of the peeling process. The cutting tool thickness affects the tool's ability to penetrate and remove the peel without damaging the flesh beneath it. A thinner cutting tool may provide a cleaner cut, reducing the amount of useful flesh lost, while a thicker tool may necessitate more force and could lead to undesirable bruising or damage to the tuber. This balance is essential for achieving optimal recovery rates.

From the established statistical inference, the predictive model obtained from the summation of components parameters resulted in higher R^2 result of 0.9754 as compared to 0.9752 achieved from the subtraction of the components variables.

Eq. (38) has been chosen as the final model due to its superior predictive accuracy and alignment with empirical data. It effectively captures the essential relationships among the variables influencing useful flesh recovery. Therefore, the model equation that is projected to produce a better statistical inference of greater R^2 value of 0.9754 was selected as the predicted model equation for useful flesh recovery requirement for the peeler and given by the equation below:

$$U_{fr} = 0.0025\left(\frac{\tau L_t t_p}{F t_{ct}}\right) + 0.7628\left(\frac{W_p t_p}{\varphi t_{ct}}\right) + 0.2373\left(\frac{\mu t_p}{\gamma t_{ct}}\right) - 0.2184 \quad (38)$$

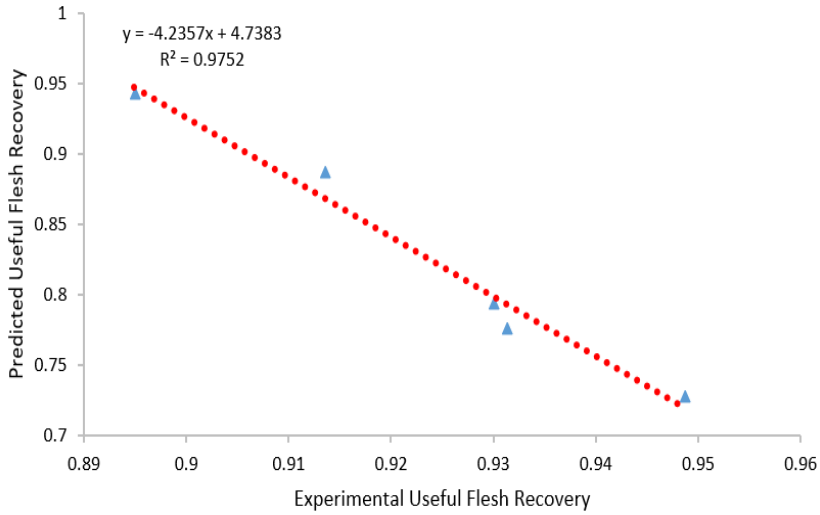

Figure 5. The correlation between the predicted and experimental useful flesh recovery for subtraction of components parameters

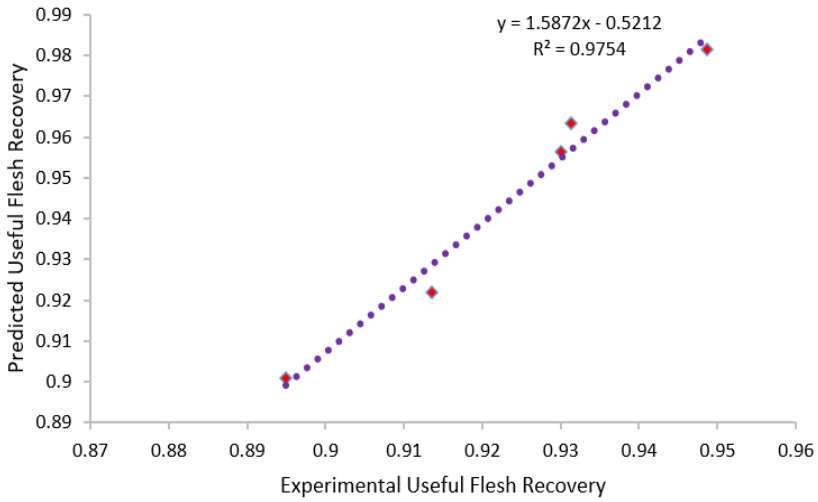

Figure 6. The correlation between the predicted and experimental useful flesh recovery for summation of components parameters

3.2 Comparison with previous works

The predictive model for useful flesh recovery developed in this study demonstrates notable advancements when compared to some existing models in the literature. For instance, Suvanjumrat et al. [47] introduced a novel drying technique integrating forced convection solar drying and electrohydrodynamic (EHD) drying, achieving a high R^2 of 0.996 for predicting diffusion coefficients. In contrast, our model achieved a R^2 value of 0.9754, underscoring its effectiveness in predicting useful flesh recovery. Gebre et al. [30] focused on predicting draft force for ard plows in smallholder farms in Ethiopia. Utilizing dimensional analysis based on the Buckingham Pi theorem, the researchers achieved a R^2 of 0.877, indicating that their model effectively predicted draft force up to 87.70%. Although their model performed well, our model achieved a higher value, showcasing superior predictive accuracy. Tupkar and Suhane [48] focused on the Dehusking efficiency of pulses using a human-powered machine, they reported an efficiency of 80.5% with a solid mathematical model grounded in dimensional analysis. While their approach successfully addressed efficiency in a different context, our model specifically targets the complexities of cassava peeling, offering a more tailored solution for agricultural processing.

4. CONCLUSIONS

This study developed a predictive model for estimating the useful flesh recovery (U_{fr}) of cassava using dimensional analysis grounded in Buckingham's π theorem. The validated model, represented by $U_{fr} = 0.0025\left(\frac{\tau L_t t_p}{Ft_{ct}}\right) + 0.7628\left(\frac{W_p t_p}{\varphi t_{ct}}\right) + 0.2373\left(\frac{\mu t_p}{\gamma t_{ct}}\right) - 0.2184$ achieved a high R^2 (0.9754) with RMSE value of 0.01, indicating robust accuracy in predicting useful flesh recovery. Engineers and manufacturers can leverage this model for practical applications, such as machine calibration and prototype testing, leading to enhanced design efficiency and reduced experimental costs. By optimizing peeling processes, the model can contribute significantly to operational efficiency and economic benefits, minimizing waste and increasing recovery rates during cassava processing.

However, the model has limitations, particularly regarding its applicability to different cassava varieties, machine types, and varying environmental conditions. Future work should focus on validating the model across diverse cassava varieties and exploring additional influencing variables, such as tuber age and moisture content. Integrating artificial intelligence models could further refine predictions and adapt the model to

real-time processing conditions, enhancing its utility in agricultural engineering.

ACKNOWLEDGMENT

The authors appreciate the support of Tshwane University of Technology, Faculty of Engineering and Built Environment, Department of Mechanical and Mechatronics Engineering, Pretoria, South Africa in this study.

REFERENCES

[1] Oyedele S.T., Ngoddy P.O., Kilanko O., Leramo R.O. (2019). Design and fabrication of a wet mechanical brushing unit for lye pre-treated cassava root. Journal of Physics: Conference Series, 1378: 022083. https://doi.org/10.1088/1742-6596/1378/2/022083

[2] Adegoke, A., Oke, M., Oriola, K., Adekoyeni, O., Sanni, L. (2023). Evaluation of cassava peeling machine using dimensional analysis technique. Mindanao Journal of Science and Technology, 21(2): 1710. https://doi.org/10.61310/mjst.v21i2.1710

[3] Bouniol, A., Ceballos, H., Bello, A., Teeken, B., Olaosebikan, D.O., Owoade, D., Dufour, D. (2024). Varietal impact on women's labour, workload and related drudgery in processing root, tuber and banana crops: focus on cassava in sub-Saharan Africa. Journal of the Science of Food and Agriculture, 104(8): 4498-4513. https://doi.org/10.1002/jsfa.12936

[4] Krishnakumar, T., Sajeev, M.S., Pradeepika, C., Namrata, A.G., Sanket, J.M., Jeevarathinam, G., Muthusamy, V. (2022). Physical and mechanical properties of cassava (Manihot esculenta Crantz) cultivars: Implications for the design of mechanical peeling machines. Journal of Food Process Engineering, 45(6): e13923. https://doi.org/10.1111/jfpe.13923

[5] Amuda, Y.J., Alabdulrahman, S. (2024). Cocoa, palm tree, and cassava plantations among smallholder farmers: Toward policy and technological efficiencies for sustainable socio-economic development in Southern Nigeria. Sustainability, 16(2): 477. https://doi.org/10.3390/su16020477

[6] Elsheikh, A.H., Shanmugan, S., Sathyamurthy, R., Thakur, A.K., Issa, M., Panchal, H., Sharifpur, M. (2022). Low-cost bilayered structure for improving the performance of solar stills: Performance/cost analysis and water yield prediction using machine learning. Sustainable Energy Technologies and Assessments, 49: 101783. https://doi.org/10.1016/j.seta.2021.101783

[7] Elsheikh, S.A., El-Anwar, M.I., Hong, T., Bourauel, C., Alhotan, A., Anany, N.M., Elshazly, T.M. (2025). Biomechanical analysis of various connector designs of dental implant complex: A numerical finite element study. International Dental Journal, 75(4): 100873. https://doi.org/10.1016/j.identj.2025.100873

[8] Dumka, P., Pawar, P.S., Sauda, A., Shukla, G., Mishra, D.R. (2022). Application of He's homotopy and perturbation method to solve heat transfer equations: A python approach. Advances in Engineering Software, 170: 103160. https://doi.org/10.1016/j.advengsoft.2022.103160

[9] Keshtkar, M., Eslami, M., Jafarpur, K. (2020). A novel procedure for transient CFD modeling of basin solar stills: Coupling of species and energy equations. Desalination, 481: 114350. https://doi.org/10.1016/j.desal.2020.114350

[10] Dhiman, N., Chauhan, A., Tamsir, M., Chauhan, A. (2020). Numerical simulation of Fisher's type equation via a collocation technique based on re-defined quintic B-splines. Multidiscipline Modeling in Materials and Structures, 16(5): 1117-1130. https://doi.org/10.1108/MMMS-09-2019-0166

[11] Lee, J.C., Bang, K.S., Yu, S.H., Choi, W.S., Ko, S. (2020). Similarity analysis of thermal-fluid flow for thermal testing using scaled-down model of spent fuel storage cask. Annals of Nuclear Energy, 149: 107791. https://doi.org/10.1016/j.anucene.2020.107791

[12] Kumar, S., Chauhan, R.P., Momani, S., Hadid, S. (2024). Numerical investigations on COVID-19 model through singular and non-singular fractional operators. Numerical Methods for Partial Differential Equations, 40(1): e22707. https://doi.org/10.1002/num.22707

[13] Fan, C., Li, L., Liu, G., Yang, X., Song, W., Guo, L., Wang, R. (2025). Numerical analysis of the stability and minimum required strength of sill mats considering creep behavior of rock mass. International Journal of Minerals, Metallurgy and Materials, 32(7): 1471-1482. https://doi.org/10.1007/s12613-024-3029-y

[14] Obiki-Osafiele, A.N., Efunniyi, C.P., Abhulimen, A.O., Osundare, O.S., Agu, E.E., Adeniran, I.A. (2024). Theoretical models for enhancing operational efficiency through technology in Nigerian businesses. International Journal of Applied Research in Social Sciences, 6(8): 1969-1989. https://doi.org/10.51594/ijarss.v6i8.1478

[15] Flaga, A. (2016). Basic principles and theorems of dimensional analysis and the theory of model similarity of physical phenomena. Czasopismo Techniczne, pp. 242-272.

[16] Martínez-Rojas, J.A., Fernández-Sánchez, J.L. (2023). Combining dimensional analysis with model based systems engineering. Systems Engineering, 26(1): 71-87. https://doi.org/10.1002/sys.21646

[17] Bahrami M., Yovanovich M.M., Culham J.R. (2006): Pressure drop of fully developed laminar flow in rough microtubes. Journal of Fluid Engineering, 128(3): 632-637. https://doi.org/10.1115/1.2175171

[18] Asonye, U.G., Nwakuba, N.R., Asoegwu, S.N. (2018). Numerical and experimental studies on the cutting energy requirements of okra (Abelmoschus esculentus L.). Arid Zone Journal of Engineering, Technology and Environment, 14(SP.i4): 20-36.

[19] Baruah, D.C., Panesar, B.S. (2005). Energy requirement model for a combine harvester, Part I: Development of component models. Biosystems Engineering, 90(1): 9-25. https://doi.org/10.1016/j.biosystemseng.2004.08.017

[20] Teske, M.E., Barry, J.W., Ekblad, R.B. (1991). Preliminary sensitivity study of aerial application inputs for FSCBG 4.0. American Society of Agricultural Engineers, Paper No. 91 - 1052.

[21] Gorial, B.Y., O'callaghan, J.R. (1991). Separation of grain from straw in a vertical air stream. Journal of Agricultural Engineering Research, 48: 111-122. https://doi.org/10.1016/0021-8634(91)80008-3

[22] McRandal, D.M., McNulty, P.B. (1978). Impact cutting behaviour of forage crops I. Mathematical models and laboratory tests. Journal of Agricultural Engineering

Research, 23(3): 313-328. https://doi.org/10.1016/0021-8634(78)90104-X
[23] Ferraz, A.C.O., Mittal, G.S., Bilanski, W.K., Abdullah, H.A. (2007). Mathematical modeling of laser based potato cutting and peeling. BioSystems, 90(3): 602-613. https://doi.org/10.1016/j.biosystems.2007.01.004
[24] Somsen, D., Capelle, A., Tramper, J. (2004). Manufacturing of par-fried French-fries: Part 2: Modelling yield efficiency of peeling. Journal of Food Engineering, 61(2): 199-207. https://doi.org/10.1016/S0260-8774(03)00093-1
[25] Aglawe, K.R., Yadav, R.K., Thool, S.B. (2022). Development of a mathematical model for prediction of heat transfer coefficient in micro-channel heat sink. Materials Today: Proceedings, 54: 753-757. https://doi.org/10.1016/j.matpr.2021.11.070
[26] Reddy, G.M., Reddy, V.D. (2014). Theoretical investigations on dimensional analysis of ball bearing parameters by using Buckingham Pi-theorem. Procedia Engineering, 97: 1305-1311. https://doi.org/10.1016/j.proeng.2014.12.410
[27] Polverino, P., Bove, G., Sorrentino, M., Pianese, C., Beretta, D. (2019). Advancements on scaling-up simulation of proton exchange membrane fuel cells impedance through Buckingham Pi theorem. Applied Energy, 249: 245-252. https://doi.org/10.1016/j.apenergy.2019.04.067
[28] Khafajah, H., Ali, M.I.H., Thomas, N., Janajreh, I., Arafat, H.A. (2022). Utilizing Buckingham Pi theorem and multiple regression analysis in scaling up direct contact membrane distillation processes. Desalination, 528: 115606. https://doi.org/10.1016/j.desal.2022.115606
[29] Ogunnigbo, C.O., Adetan, D.A., Morakinyo, T.A. (2022). A study on the mathematical model for predicting the peel removal efficiency of a cassava peeler. Research in Agricultural Engineering, 68(1): 18-26. https://doi.org/10.17221/32/2021-RAE
[30] Gebre, T., Abdi, Z., Wako, A., Yitbarek, T. (2023). Development of a mathematical model for determining the draft force of ARD plow in silt clay soil. Journal of Terramechanics, 106: 13-19. https://doi.org/10.1016/j.jterra.2022.11.004
[31] Almehmadi, F.A., Najib, A., Al-Ansary, H. (2024). Prediction of key performance indicators of multi-effect vacuum membrane distillation systems integrated with PVT and Organic Rankin Cycle. Case Studies in Thermal Engineering, 61: 105080. https://doi.org/10.1016/j.csite.2024.105080
[32] Fox, R.W., McDonald, A.T. (1992): Introduction to Fluid Mechanics. John Wiley and Sons, New York.
[33] Conejo, A.N. (2021). Fundamentals of Dimensional Analysis. Theory and Applications in Metallurgy. Springer, Singapore. https://doi.org/10.1007/978-981-16-1602-0
[34] Ndirika V.I.O. (1997): Modeling the performance of selected stationary grain threshers. PhD. Dissertation, Department of Agricultural Engineering, Ahmadu Bello University Zaria, Nigeria.
[35] Babashani, B. (2008). Mathematical modeling of the spray penetration and deposition on orchard tree canopies. PhD. Thesis. Ahmadu Bello University, Nigeria.
[36] Simonyan, K.J., Yiljep, Y.D., Mudiare, O.J. (2006). Modeling the grain cleaning process of a stationary sorghum thresher. Agricultural Engineering International: CIGR Journal, 3: 1-16.
[37] Ndirika, V.I.O. (2006): A mathematical model for predicting output capacity of selected stationary grain threshers. Agricultural Mechanization in Asia, Africa and Latin America (AMA), 36: 9-13.
[38] Ndukwu, M.C., Asoegwu, S.N. (2011): A mathematical model for predicting the cracking efficiency of vertical-shaft centrifugal palm nut cracker. Research in Agricultural Engineering, 57(3): 110-115. https://doi.org/10.17221/38/2010-RAE
[39] Asoegwu, S.N., Agbetoye, L.A.S., Ogunlowo, A.S. (2010). Modeling flow rate of Egusi- melon (Colocynthis citrullus) through circular horizontal hopper orifice. Advances in Science and Technology, 4(1): 35-44.
[40] Shefii, S., Upadhyaya, S.K., Garret, R.E. (1996). The importance of experimental design to the development of empirical prediction equations: A case study. Transaction of American Society of Agricultural and Bio-resources Engineers. 39: 377-384. https://doi.org/10.13031/2013.27512
[41] Adetan, D.A., Adekoya L.O., Aluko, O.L. (2003): Characterization of some properties of cassava root tubers. Journal of Food Engineering. 59: 349-353. https://doi.org/10.1016/S0260-8774(02)00493-4
[42] Aji, I.S., Emmanuel, M.U., Abdulrahman, S.A., Franklyn, O.F. (2016): Development of an electrically operated cassava peeling and slicing machine. Arid Zone Journal of Engineering, Technology and Environment, 12: 40-48.
[43] Nwagugu, N.I., Okonkwo, W.I. (2009): Experimental determination of comprehensive strength of sweet cassava (Manihot Esculanta). In Proceedings of the 9th International conference of West African Society of Agric. Engineers and Nigerian Institution of Agric. Engineers, pp. 191-197.
[44] Kolawole, O.P., Agbetoye, L.A.S., Ogunlowo, A.S. (2007). Strength and elastic properties of cassava tuber. International Journal of Food Engineering, 3(5): 1225. https://doi.org/10.2202/1556-3758.1225
[45] Mohammed, U.S. (2002): Performance modeling of the cutting process in sorghum harvesting. Ahmadu Bello University, Nigeria.
[46] Rendón-Castrillón, L., Ramírez-Carmona, M., Ocampo-López, C., Gómez-Arroyave, L. (2021). Mathematical model for scaling up bioprocesses using experiment design combined with Buckingham Pi theorem. Applied Sciences, 11(23): 11338. https://doi.org/10.3390/app112311338
[47] Suvanjumrat, C., Chuckpaiwong, I., Chookaew, W., Priyadumkol, J. (2024). Assessment of the pineapple drying with a forced convection solar-electrohydrodynamic dryer. Case Studies in Thermal Engineering, 59: 104582. https://doi.org/10.1016/j.csite.2024.104582
[48] Tupkar, A., Suhane, R. (2022). Establishment of mathematical model to predict the dehulling efficiency in miniature pulse splitter machine energized by human powered flywheel motor using dimensional analysis. Materials Today: Proceedings, 65: 3567-3572. https://doi.org/10.1016/j.matpr.2022.06.149

NOMENCLATURE

F Penetration force, $N.mm^{-1}$
L Length, mm
U Useful
W Weight proportion, %

Greek symbols

ω Tuber rotational speed, rpm
τ Peel share stress, $N.\ mm^{-2}$
γ Tuber shape, dimensionless
φ Moisture content of peel, dimensionless
μ Coefficient of friction

Subscripts

t Tuber
fr Flesh recovery
p Peel
ct Peeling tool